

Phenolic esters with potential anticancer activity - the structural variable

Nelson F. L. Machado · Rita Calheiros ·
Sónia M. Fiuza · Fernanda Borges ·
Alexandra Gaspar · Jorge Garrido · Maria P. Marques

Received: 10 November 2006 / Accepted: 22 January 2007 / Published online: 6 March 2007
© Springer-Verlag 2007

Abstract The conformational preferences of several potential anticancer dihydroxycinnamic esters with a variable length alkyl chain were studied by quantum-mechanical (DFT) calculations (both for the isolated molecule and for aqueous solutions). The orientation of the hydroxyl ring substituents and of the alkyl ester moiety relative to the carbonyl group showed these to be the most determinant factors for the overall stability of this type of phenolic systems, strongly dependent on an effective π -electron delocalization. Compared to the parent caffeic acid (dihydroxycinnamic acid), esterification was found to lead to a higher conformational freedom, and to affect mainly the energy barrier corresponding to the (O=C)-OR internal rotation. No particular differences were verified to occur upon lengthening of the ester alkyl chain, except when this is branched instead of linear. The vibrational spectra of the

whole series of compounds were simulated, based on their calculated harmonic vibrational frequencies, and a preliminary assignment was performed.

Keywords Dihydroxycinnamates · Anticancer · Density functional theory · Conformational analysis · Theoretical vibrational spectra

Introduction

Antioxidants are hypothesized to play an important role in disease prevention, since they may be able to avoid oxidative damage caused by reactive oxidant species to vital biomolecules, such as DNA, lipids and proteins. This type of oxidative mechanism is widely accepted to be involved in numerous pathological processes, such as cardiovascular and neurodegenerative diseases, inflammation and carcinogenesis [1–4]. A high number of phenolic derivatives (e.g., esters and amides) can act as antioxidants, with varying levels of efficacy [5–7]. In particular, cinnamic acid and its derivatives are known to display interesting antioxidant and antitumour properties. Actually, numerous reports on the antioxidant and anticancer activities of structurally modified cinnamic acids are to be found in the literature [8–11]. Some of these compounds, with special emphasis on the esters comprising an intermediate length alkyl chain, were found to display significant antiproliferative effects towards human cancer cells, along with a low toxicity against non-neoplastic cells [9–12]. Caffeic acid phenethyl ester (CAPE), for instance, is a component of honeybee hives propolis that has recently been shown to have both immunomodulatory and anticarcinogenic capacity [13–16]. Due to their natural origin and to their presence in food and food-derived products,

N. F. L. Machado · R. Calheiros · S. M. Fiuza · A. Gaspar
Unidade I&D “Química-Física Molecular”,
Faculdade de Ciências e Tecnologia,
Universidade de Coimbra,
3000 Coimbra, Portugal

F. Borges
Departamento Química Orgânica, Faculdade de Farmácia,
Universidade do Porto,
4050-047 Porto, Portugal

J. Garrido
Departamento Engenharia Química,
Instituto Superior de Engenharia do Porto,
4200-072 Porto, Portugal

M. P. Marques (✉)
Departamento Bioquímica, Faculdade de Ciências e Tecnologia,
Universidade de Coimbra,
Apartado 3126,
3001-401 Coimbra, Portugal
e-mail: pmc@ci.uc.pt

these systems are of interest for the development of new antioxidants with both preventive and therapeutic aims. Thus, the evaluation and interpretation (at the molecular level) of the biological activity of phenolic compounds is presently the object of intense research [2, 3, 17].

Several studies have recently been carried out in order to find new leader compounds—e.g., structurally based on benzoic and cinnamic acids [8, 11]—suitable for the development of new chemopreventive and/or chemotherapeutic agents. Due to their natural origin and to their presence in food and food-derived products, this group of phenolic compounds is presently considered to be the most interesting one for drug design.

Marked structure–activity relationships (SARs) were found to rule the biological role of phenolic systems, namely the number and relative position of the ring hydroxyl substituents, as well as the chemical nature and spatial orientation of the linker between the ring and the carboxylate moiety (e.g., saturated vs unsaturated) and of the ester alkyl chain (e.g., linear vs branched). Therefore, the knowledge of these conformational preferences is of the utmost importance for the understanding and/or prediction of the biochemical function of this kind of system, and for the rational design of new antioxidant/anticancer agents [2, 3, 9–11, 17]. However, even though there is a wealth of data on the relevance of phenols as growth-inhibiting and cytotoxic compounds, the correlation between this activity and chemical structure is far from understood.

The present work reports a conformational analysis, by quantum mechanical calculations, at the Density Functional Theory (DFT) level (both for the isolated molecule and for aqueous solutions), of the variable length dihydroxycinnamic esters (caffeic acid derivatives): methyl *trans*-3-(3,4-dihydroxyphenyl)-2-propenoate (methyl caffeate, MC), ethyl *trans*-3-(3,4-dihydroxyphenyl)-2-propenoate (ethyl caffeate, EC), propyl *trans*-3-(3,4-dihydroxyphenyl)-2-propenoate (propyl caffeate, PC), isopropyl *trans*-3-(3,4-dihydroxyphenyl)-2-propenoate (isopropyl caffeate, IPC), butyl *trans*-3-(3,4-dihydroxyphenyl)-2-propenoate (butyl caffeate, BC), octyl *trans*-3-(3,4-dihydroxyphenyl)-2-propenoate (octyl caffeate, OC) and dodecyl *trans*-3-(3,4-dihydroxyphenyl)-2-propenoate (dodecyl caffeate, DC). The corresponding experimental Raman data will be reported briefly, and completely assigned in the light of the presently discussed theoretical results (manuscript in preparation).

Methods

The calculations were performed using the GAUSSIAN 03W program [18], within the DFT approach, in order to properly account for the electron correlation effects (par-

ticularly important in this kind of conjugated systems). The widely employed hybrid method denoted by B3LYP, which includes a mixture of HF and DFT exchange terms and the gradient-corrected correlation functional of Lee, Yang and Parr [19, 20], as proposed and parametrized by Becke [21, 22], was used, along with the double-zeta split valence basis set 6-31G** [23].

Molecular geometries were fully optimized by the Berny algorithm, using redundant internal coordinates [24]: the bond lengths to within ca. 0.1 pm and the bond angles to within ca. 0.1°. The final root-mean-square (rms) gradients were always less than 3×10^{-4} hartree.bohr⁻¹ or hartree.radian⁻¹. No geometrical constraints were imposed on the molecules under study.

For each molecule studied, a full geometry optimisation was performed, and calculation of the harmonic vibrational frequencies was carried out (at the same level of theory) in order to confirm the convergence to minima in the potential energy surface and to obtain the corresponding theoretical vibrational pattern. The relative energies and populations (Boltzman distribution, at 298.15 K) were calculated for all conformers, using the sum of the electronic and zero-point energies.

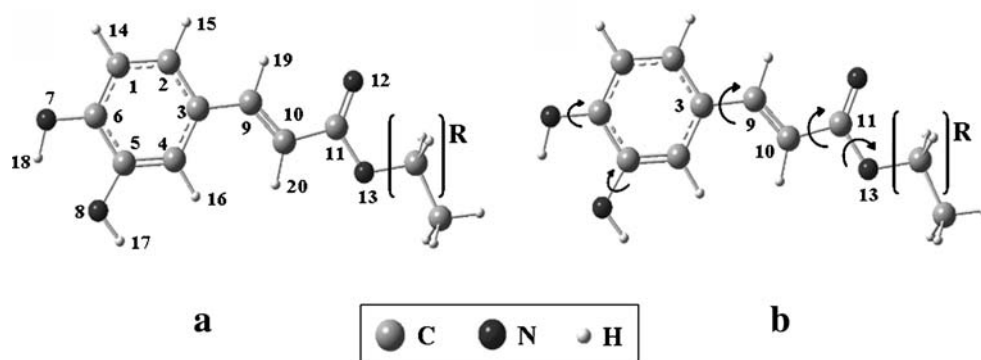
The solvent effect (water) was simulated by performing Self-Consistent Reaction Field (SCRf) calculations. A continuum model—the Integral Equation Formalism (IEF) [25–27] version of Tomasi's Polarized Continuum Model (PCM) [28, 29]—was used. This approach defines the molecular cavity as the union of a series of interlocking spheres centered on the distinct atoms of the system.

Results and discussion

A conformational study, by quantum mechanical calculations, was performed for the series of variable length dihydroxycinnamates (alkyl caffeates) containing methyl, ethyl, propyl, isopropyl, butyl, octyl and dodecyl alkyl substituents groups (Fig. 1a). An extensive conformational analysis was undertaken for methyl, ethyl and isopropyl caffeates, the corresponding optimized geometries, relative energies and populations at room temperature having been obtained for all the conformers found for these systems. The results thus obtained were extrapolated to the longer esters of the series, for which only the most stable geometries were then considered in the calculations. A frequency analysis was also performed yielding the theoretical Raman spectra, and an preliminary assignment of these vibrational modes was carried out.

The effect of the following structural parameters on the overall stability of the molecules under study was determined (Fig. 1b): (1) localisation of the alkyl ester moiety with respect to the aromatic ring (rotation around C₃–C₉);

Fig. 1 Schematic representation of the dihydrocinnamic esters studied in the present work and of the main internal rotations affecting the overall stability of the molecules. ($R=(CH_2)_n$, $n=0,1,2,3,7,11$ for MC, EC, PC, BC, OC and DC, respectively; $R=(CHCH_3)$ for IPC. The atom numbering is included, with the exception of the alkyl ester group)



(2) orientation of the alkyl ester group relative to the carbonyl (rotation around $C_{11}-O_{13}$), either *S-cis* or *S-trans*; (3) relative orientation of the OH ring substituents on the aromatic nucleus; (4) position of these hydroxyl group(s) relative to the plane of the ring—either in-plane or out-of-plane; and (5) relative orientation of the carbonyl and ring OH groups (rotation around $C_{10}-C_{11}$), either *syn* or *anti*. Only the *trans* isomers—displaying an opposite orientation of the ring and the $C=O$ group relative to the bridging chain double bond—were considered, since they were previously reported to be largely stabilized relative to the *cis* molecules, irrespective of the number of ring substituents [11].

For all the systems presently investigated, the most stable conformers were found to display a planar or quasi-planar geometry, which corresponds to a maximum stabilization due to an effective π -electron delocalization

between the aromatic ring and the $C=O$ and $C=C$ double bonds. Regarding the variable length of the alkyl ester group and the pendant carbon chain, a zig-zag conformation was verified as yielding the lowest energy structures.

An identical orientation of the aromatic OH substituents (coplanar with the ring) was found to be strongly favored, since it minimizes steric repulsions and enables the formation of highly stabilizing medium strength intramolecular $(O)H \cdots O$ interactions— $d_O \cdots H=211-214$ pm (Figs. 3, 5 and 7). Although some stable geometries were obtained for opposite positions of these ring hydroxyls, no energy minima were found when they were directed towards each other (due to the strong steric H-H repulsion).

Internal rotation around $C_{11}-O_{13}$ —defining the relative position of the alkyl ester group and the carbonyl (Fig. 1b)—was found to be the most determinant factor for the overall stability of this type of systems. In fact, those conformers

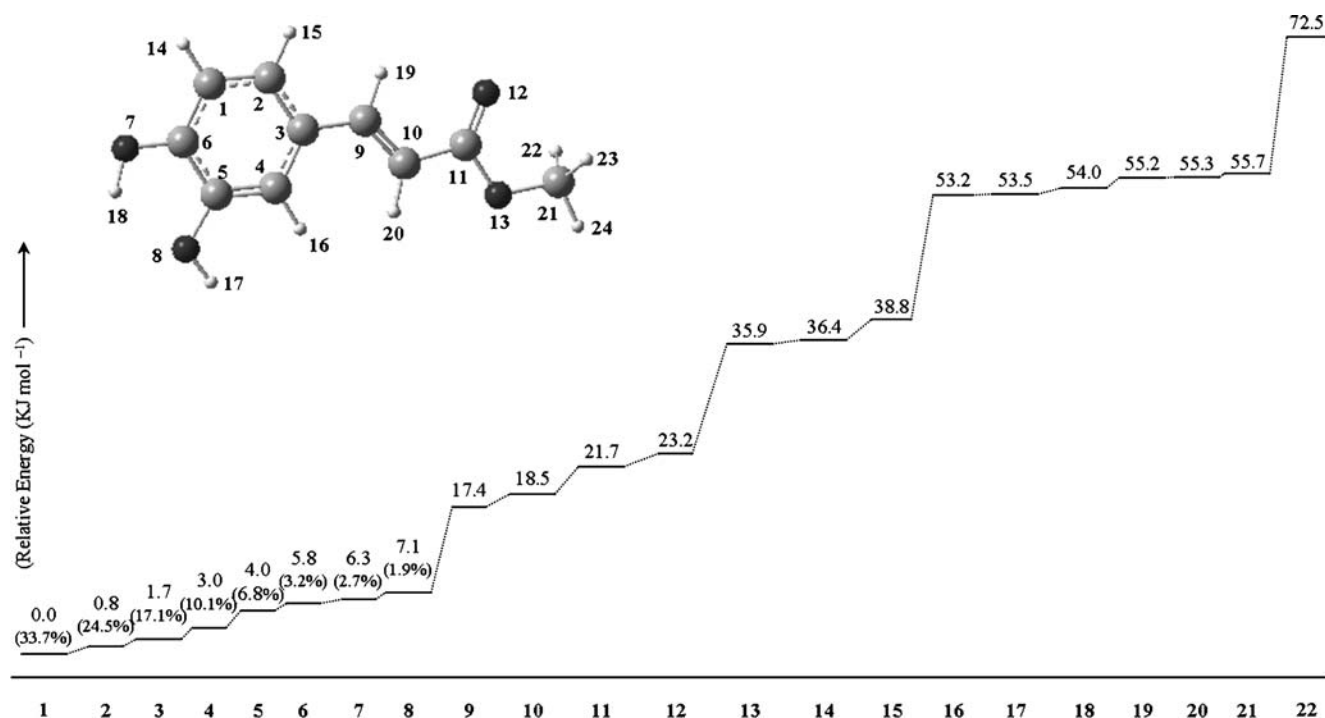


Fig. 2 Schematic representation of the calculated (B3LYP/6-31G**) conformational energies (and populations, at 25 °C) for MC. The atom numbering is included. The numbers in the xx' axis refer to the different calculated conformers

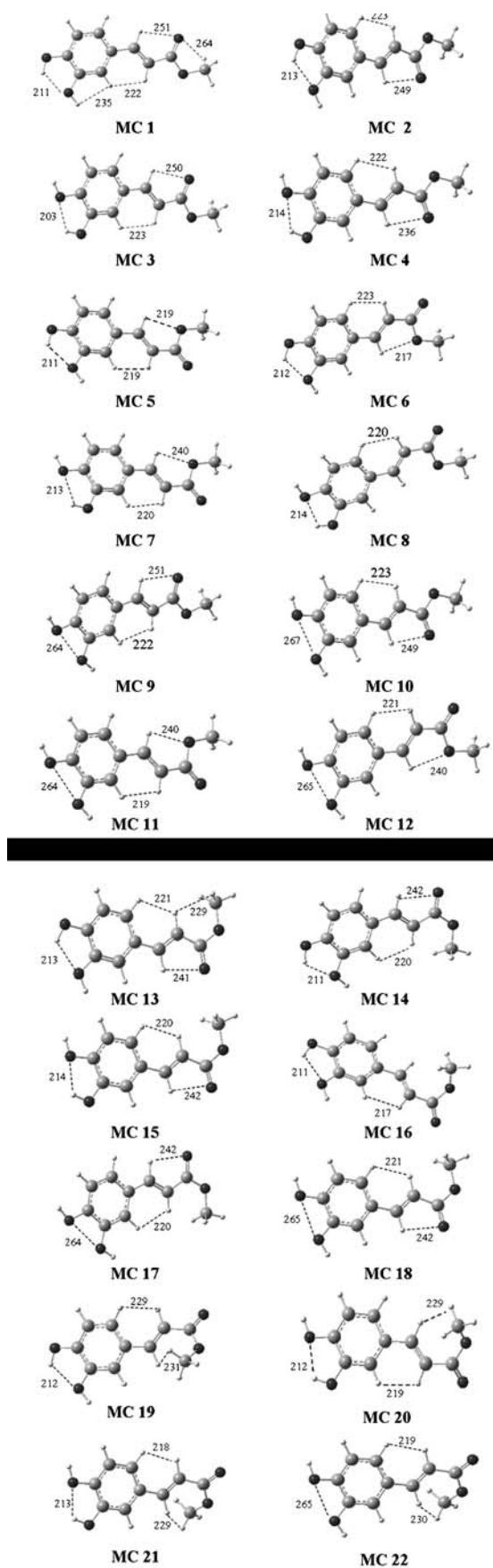


Fig. 3 Representation of the several conformers calculated for MC displaying (C)H \cdots :O and (O)H \cdots :O intramolecular interactions. B3LYP/6-31G** level of calculation. Intramolecular distances are represented in pm

with an alkyl ester *S-trans* orientation were shown to be greatly unfavored as compared to their *S-cis* counterparts.

Moreover, the most stable conformations display an *anti* orientation of the carbonyl and ring substituent groups (Fig. 1). This may be explained in terms of the π -electron delocalization, a recognisably important effect for the stabilization of this kind of molecule, which was shown to be more efficient for the *anti* conformation when two OH's are bound to the aromatic ring (one in the *para* position relative to the side chain and the other in *meta*) in previous studies on similar phenolic systems, namely caffeic acid (3-(3,4-dihydroxyphenyl)-2-propenoic acid) [30]. For analogous trihydroxylated molecules such as THPPE (3-(3,4,5-trihydroxyphenyl)-2-propenoic acid) and ETHPPE (ethyl 3-(3,4,5-trihydroxyphenyl)-2-propenoate), in turn, the *syn* conformers were reported to be favored [11, 31].

The present conformational analysis rendered 22 conformers for MC (Figs. 2 and 3), 21 for EC (Figs. 4 and 5) and 17 for IPC (Figs. 6 and 7). As previously discussed, the two major parameters affecting the stability of these systems were found to be the relative orientation of the alkyl ester and the carbonyl groups (either *S-cis* or *S-trans*, as a result of $C_{11}-O_{13}$ internal rotation), and the position of the OH ring substituents with respect to the aromatic plane. Table 1 comprises the calculated optimized geometrical parameters for the most stable conformer of methyl (MC), ethyl (EC) and isopropyl caffeates (IPC). (Tables containing the optimized geometrical parameters for the other esters studied are available from the authors upon request.)

For all the esters studied, the *S-cis* conformations were clearly stabilized relative to the *S-trans* ones—conformers MC1 to MC12 versus MC13 to MC22 (Figs. 2 and 3), EC1 to EC12 versus EC13 to EC21 (Figs. 4 and 5), and IPC1 to IPC12 versus IPC13 to IPC17 (Figs. 6 and 7). The most stable *S-trans* conformer obtained for IPC (IPC13), for instance, is 36.7 kJ mol^{-1} higher than the corresponding lowest energy *S-cis* species (IPC2). In fact, an *S-trans* orientation of the ester alkyl group relative to the carbonyl was verified to be energetically more unfavorable than an opposite position of the ring OH groups: e.g., MC1 ($\Delta E=0$) and MC9 ($\Delta E=17.4 \text{ kJ mol}^{-1}$) versus MC1 ($\Delta E=0$) and MC14 ($\Delta E=36.4 \text{ kJ mol}^{-1}$) (Fig. 3).

The highest energy conformations calculated for methyl caffeate, MC22 ($\Delta E=72.5 \text{ kJ mol}^{-1}$) and isopropyl caffeate, IPC17 ($\Delta E=55.4 \text{ kJ mol}^{-1}$) display the combination of the two destabilizing factors—an opposite orientation of the ring hydroxyls and an *S-trans* conformation of the ester alkyl group relative to C=O (Figs. 3 and 7). As for ethyl caffeate, the less stable arrangement (EC21, $\Delta E=53.9 \text{ kJ mol}^{-1}$)

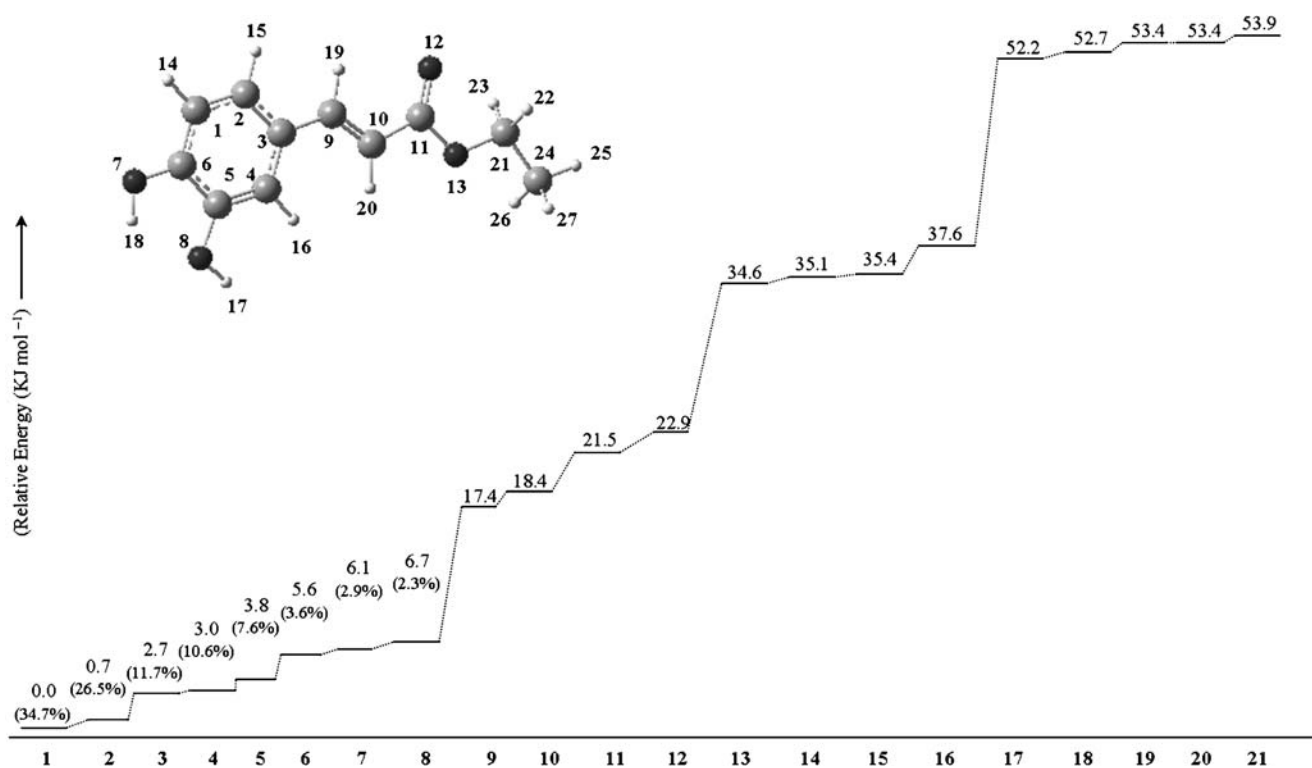


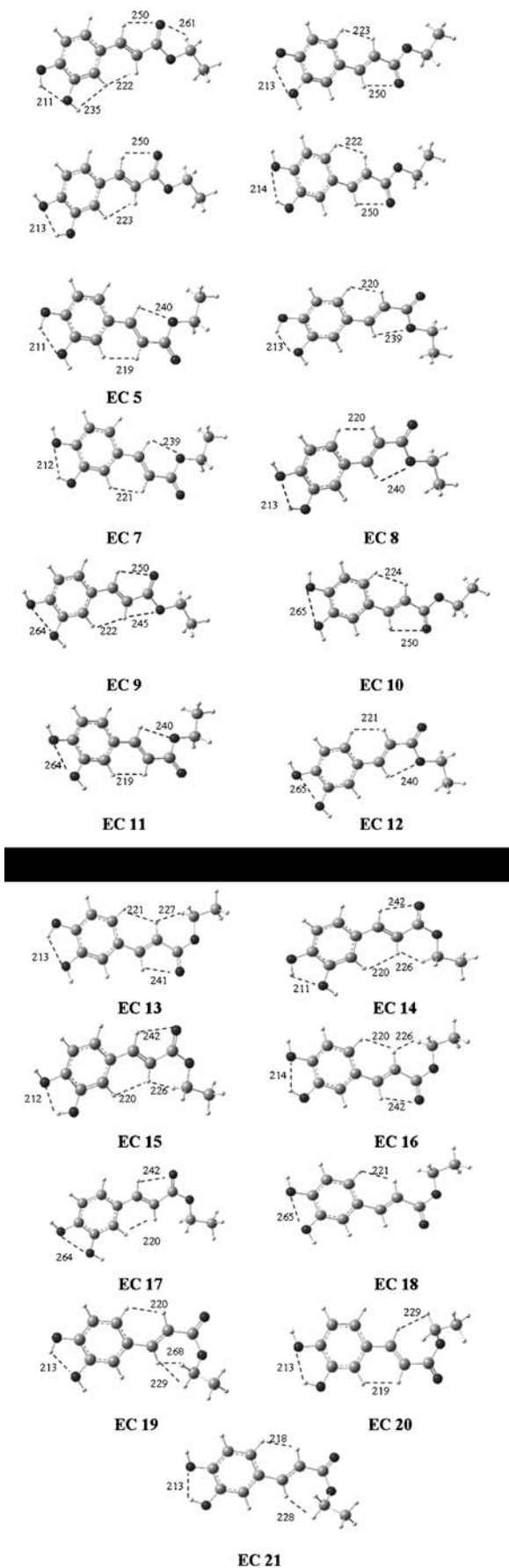
Fig. 4 Schematic representation of the calculated (B3LYP/6-31G**) conformational energies (and populations, at 25 °C) for EC. The atom numbering is included. The numbers in the xx' axis refer to the different calculated conformers

mol^{-1}) was calculated to be the one displaying a *syn* relative orientation of the ring hydroxyls and the carbonyl group, an *S-trans* conformation, and a combination of unfavourable dihedrals ($\text{C}_2\text{C}_3\text{C}_9\text{C}_{10}$)= 0° and ($\text{C}_9\text{C}_{10}\text{C}_{11}\text{O}_{12}$)= 180° (Fig. 5). For the *S-cis* geometries the calculated relative energy values were identical for the three esters (Figs. 2, 4 and 6).

The most favorable combination of the ($\text{C}_2\text{C}_3\text{C}_9\text{C}_{10}$) and ($\text{C}_9\text{C}_{10}\text{C}_{11}\text{O}_{12}$) dihedrals was found to be 180° and 0° , respectively, which explains the following stability order for MC (Figs. 2 and 3): MC1 ($\text{C}_2\text{C}_3\text{C}_9\text{C}_{10}$)= 180° and ($\text{C}_9\text{C}_{10}\text{C}_{11}\text{O}_{12}$)= 0° , $\Delta E=0$; MC2 ($\text{C}_2\text{C}_3\text{C}_9\text{C}_{10}$)= 0° and ($\text{C}_9\text{C}_{10}\text{C}_{11}\text{O}_{12}$)= 0° , $\Delta E=0.8 \text{ kJ mol}^{-1}$; MC5 ($\text{C}_2\text{C}_3\text{C}_9\text{C}_{10}$)= 180° and ($\text{C}_9\text{C}_{10}\text{C}_{11}\text{O}_{12}$)= 180° , $\Delta E=4.0 \text{ kJ mol}^{-1}$; and MC6 ($\text{C}_2\text{C}_3\text{C}_9\text{C}_{10}$)= 0° and ($\text{C}_9\text{C}_{10}\text{C}_{11}\text{O}_{12}$)= 180° , $\Delta E=5.8 \text{ kJ mol}^{-1}$. For the *S-trans* geometries (with an *anti* orientation of the carbonyl relative to the ring OH's): MC14 ($\text{C}_2\text{C}_3\text{C}_9\text{C}_{10}$)= 180° and ($\text{C}_9\text{C}_{10}\text{C}_{11}\text{O}_{12}$)= 0° , $\Delta E=36.4 \text{ kJ mol}^{-1}$; MC15 ($\text{C}_2\text{C}_3\text{C}_9\text{C}_{10}$)= 0° and ($\text{C}_9\text{C}_{10}\text{C}_{11}\text{O}_{12}$)= 0° , $\Delta E=38.8 \text{ kJ mol}^{-1}$; MC19 ($\text{C}_2\text{C}_3\text{C}_9\text{C}_{10}$)= 0° and ($\text{C}_9\text{C}_{10}\text{C}_{11}\text{O}_{12}$)= 180° , $\Delta E=55.2 \text{ kJ mol}^{-1}$; MC20 ($\text{C}_2\text{C}_3\text{C}_9\text{C}_{10}$)= 180° and ($\text{C}_9\text{C}_{10}\text{C}_{11}\text{O}_{12}$)= 180° , $\Delta E=55.3 \text{ kJ mol}^{-1}$. The same considerations apply for an opposite orientation of the ring OH's, both for the *S-cis* and *S-trans* conformers (Figs. 2 and 3): MC9 ($\text{C}_2\text{C}_3\text{C}_9\text{C}_{10}$)= 180° and ($\text{C}_9\text{C}_{10}\text{C}_{11}\text{O}_{12}$)= 0° , $\Delta E=17.4 \text{ kJ mol}^{-1}$; MC10 ($\text{C}_2\text{C}_3\text{C}_9\text{C}_{10}$)= 0° and ($\text{C}_9\text{C}_{10}\text{C}_{11}\text{O}_{12}$)= 0° , $\Delta E=18.5 \text{ kJ mol}^{-1}$; MC11 ($\text{C}_2\text{C}_3\text{C}_9\text{C}_{10}$)= 180° and ($\text{C}_9\text{C}_{10}\text{C}_{11}\text{O}_{12}$)= 180° , $\Delta E=21.7 \text{ kJ}$

mol^{-1} ; and MC12 ($\text{C}_2\text{C}_3\text{C}_9\text{C}_{10}$)= 0° and ($\text{C}_9\text{C}_{10}\text{C}_{11}\text{O}_{12}$)= 180° , $\Delta E=23.2 \text{ kJ mol}^{-1}$; MC17 ($\text{C}_2\text{C}_3\text{C}_9\text{C}_{10}$)= 180° and ($\text{C}_9\text{C}_{10}\text{C}_{11}\text{O}_{12}$)= 0° , $\Delta E=53.5 \text{ kJ mol}^{-1}$; MC18 ($\text{C}_2\text{C}_3\text{C}_9\text{C}_{10}$)= 0° and ($\text{C}_9\text{C}_{10}\text{C}_{11}\text{O}_{12}$)= 0° , $\Delta E=54.0 \text{ kJ mol}^{-1}$; and MC22 ($\text{C}_2\text{C}_3\text{C}_9\text{C}_{10}$)= 0° and ($\text{C}_9\text{C}_{10}\text{C}_{11}\text{O}_{12}$)= 180° , $\Delta E=72.5 \text{ kJ mol}^{-1}$, the latter having two destabilizing dihedral values. In fact, this highly unfavorable arrangement was only calculated to be an energy minimum for the smallest element of the series, MC. Also, a variation in the ($\text{C}_2\text{C}_3\text{C}_9\text{C}_{10}$) dihedral was shown to affect stability less significantly than a change in ($\text{C}_9\text{C}_{10}\text{C}_{11}\text{O}_{12}$): MC1 ($\text{C}_2\text{C}_3\text{C}_9\text{C}_{10}$)= 180° versus MC2 ($\text{C}_2\text{C}_3\text{C}_9\text{C}_{10}$)= 0° , $\Delta E=0.8 \text{ kJ mol}^{-1}$, as compared to MC1 ($\text{C}_9\text{C}_{10}\text{C}_{11}\text{O}_{12}$)= 180° versus MC5 ($\text{C}_9\text{C}_{10}\text{C}_{11}\text{O}_{12}$)= 0° , $\Delta E=4.0 \text{ kJ mol}^{-1}$.

The conformational behavior described above is extensive to the ethyl and isopropyl esters, except for the fact that the IPC *S-trans* geometries with ($\text{C}_2\text{C}_3\text{C}_9\text{C}_{10}$)= 0° and ($\text{C}_9\text{C}_{10}\text{C}_{11}\text{O}_{12}$)= 180° were not found to be conformers, due to the destabilizing steric hindrance between the rather bulky isopropyl group and the neighboring H atoms (Fig. 7). Moreover, the *S-trans* conformations displaying opposite ring OH's, with ($\text{C}_2\text{C}_3\text{C}_9\text{C}_{10}$)= 180° and ($\text{C}_9\text{C}_{10}\text{C}_{11}\text{O}_{12}$)= 180° , are not minima in the potential energy surface. Furthermore, while for both EC and IPC the *syn* arrangement having ($\text{C}_2\text{C}_3\text{C}_9\text{C}_{10}$)= 180° and ($\text{C}_9\text{C}_{10}\text{C}_{11}\text{O}_{12}$)= 0° was verified to be a minimum in the potential energy surface—EC15 ($\Delta E=35.4 \text{ kJ mol}^{-1}$) and IPC 15 ($\Delta E=38.0 \text{ kJ mol}^{-1}$)—for MC only the *anti*



◀ **Fig. 5** Representation of the several conformers calculated for EC displaying (C)H \cdots O and (O)H \cdots O intramolecular interactions. B3LYP/6-31G** level of calculation. Intramolecular distances are represented in pm

geometry is a conformer, for this set of dihedrals—MC14 ($\Delta E=36.4$ kJ mol $^{-1}$).

Rotation around the C $_{10}$ –C $_{11}$ bond interchanges the *anti* and *syn* geometries with respect to the relative orientation of the C=O and ring hydroxyl groups, the latter being clear unfavored. For EC, for instance: EC1 ($\Delta E=0$) versus EC5 ($\Delta E=3.8$ kJ mol $^{-1}$); EC13 ($\Delta E=34.6$ kJ mol $^{-1}$) versus EC19 ($\Delta E=53.4$ kJ mol $^{-1}$); EC16 ($\Delta E=37.6$ kJ mol $^{-1}$) versus EC21 ($\Delta E=53.9$ kJ mol $^{-1}$).

For the *S-trans* geometries of MC and EC with (C $_9$ C $_{10}$ C $_{11}$ O $_{13}$) $\neq 180^\circ$ —MC16, MC19, MC20, MC21, MC22, EC19, EC20 and EC21 (Figs. 3 and 5), tilted conformations were obtained ((C $_9$ C $_{10}$ C $_{11}$ O $_{13}$) = 34 to 36 $^\circ$, and (C $_{10}$ C $_{11}$ O $_{13}$ C $_{21}$) = 30 to 34 $^\circ$) corresponding to a maximum distance between the ester alkyl hydrogens and the neighboring H $_{19}$ atom ($d_{\text{H}} \cdots \text{H}_{19/20}=228$ to 231). For IPC, in turn, these geometries are strongly unfavored since they lead to severe steric hindrance between the isopropyl hydrogens and H $_{19}$ (Fig. 7). Actually, for the series of esters investigated these destabilizing repulsions are minimized through rotation around the O $_{13}$ –C $_{21}$ bond.

Rotation of the aromatic ring relative to the alkyl ester moiety (about the C $_3$ –C $_9$ bond) also interconvert the *anti* and *syn* conformations, the former being energetically favored when (C $_2$ C $_3$ C $_9$ C $_{10}$)=180 $^\circ$: e.g., IPC5 ($\Delta E=3.7$ kJ mol $^{-1}$) versus IPC7 ($\Delta E=6.1$ kJ mol $^{-1}$); IPC6 ($\Delta E=5.5$ kJ mol $^{-1}$) versus IPC8 ($\Delta E=6.6$ kJ mol $^{-1}$). In fact, the *syn* conformers display lower relative energies for both (C $_2$ C $_3$ C $_9$ C $_{10}$) and (C $_9$ C $_{10}$ C $_{11}$ O $_{12}$) dihedrals equal to 0 $^\circ$, either for an *S-cis* or an *S-trans* geometry: MC2 ($\Delta E=0.8$ kJ mol $^{-1}$) versus MC5 ($\Delta E=4.0$ kJ mol $^{-1}$); EC13 ($\Delta E=34.6$ kJ mol $^{-1}$) versus EC21 ($\Delta E=53.9$ kJ mol $^{-1}$); and IPC13 ($\Delta E=37.3$ kJ mol $^{-1}$) versus IPC15 ($\Delta E=38.0$ kJ mol $^{-1}$).

In general, the conformational energy profile for the homologous series of alkyl esters studied is ruled by the following factors, by decreasing order of stability (Figs. 2, 4 and 6): (1) equal orientation of the ring hydroxyls—eight lowest energy conformers; (2) opposed orientation of the ring OH's—geometries 9 to 12, corresponding to an energy gap (ΔE_{9-8}) of 10.3 to 10.8 kJ mol $^{-1}$; (3) *S-cis* versus *S-trans* conformation of the alkyl ester group relative to the carbonyl—arrangements 13 to 15 (for MC)/16 (for EC and IPC), with identically oriented ring OH's, corresponding to an energy gap of 11.7 to 14.5 kJ mol $^{-1}$; (4) for the MC and EC esters, an *S-trans* conformation combined to opposed ring hydroxyls (MC17, MC18, EC17 and EC18) or non-planar geometries (MC16, MC19, MC21, EC19, EC20 and EC21), for an energy gap of 14.4 to 14.6 kJ mol $^{-1}$; and (5)

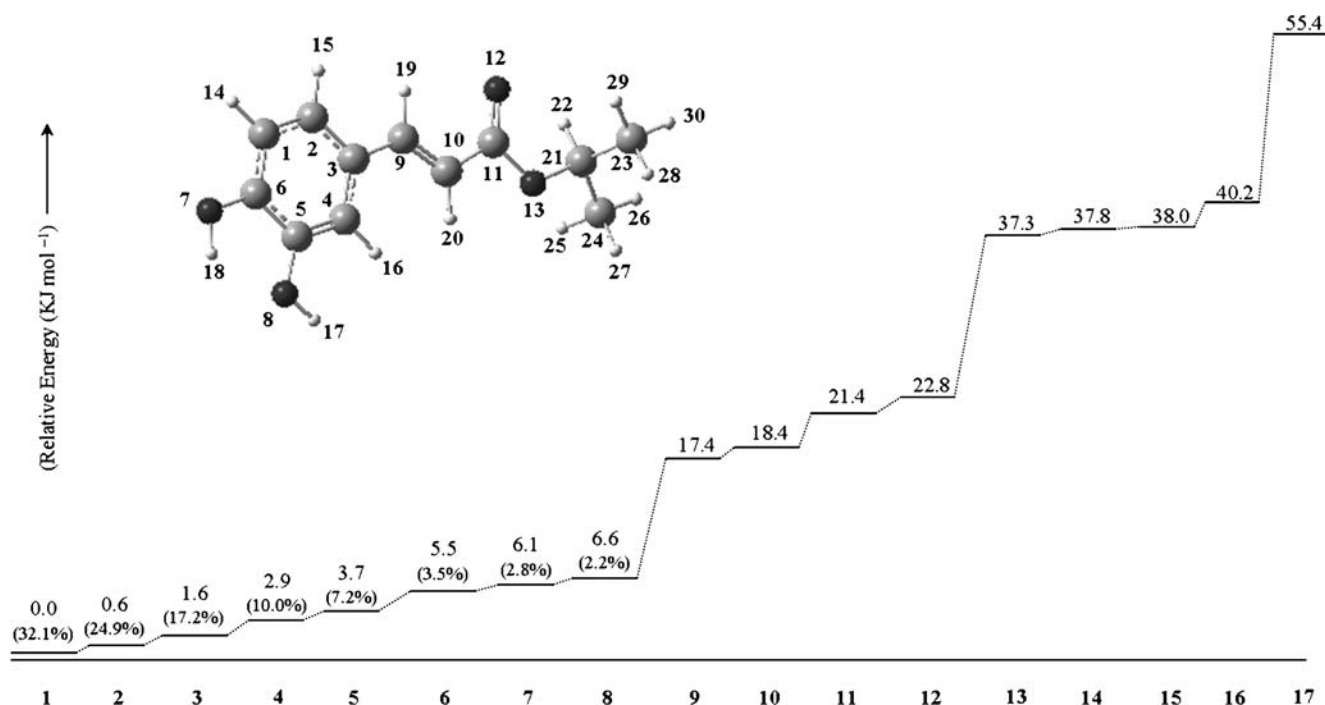


Fig. 6 Schematic representation of the calculated (B3LYP/6-31G**) conformational energies (and populations, at 25 °C) for IPC. The atom numbering is included. The numbers in the xx' axis refer to the different calculated conformers

for MC and IPC, an *S-trans* conformation coupled to opposed ring OH's, and ($C_9C_{10}C_{11}O_{12}$) and ($C_2C_3C_9C_{10}$) dihedrals equal to 180° and 0° , respectively, for an energy gap of 15.2 to 16.8 kJ mol⁻¹.

The same number of *S-cis* arrangements (12) was obtained for MC, EC and IPC, irrespective of the nature of their ester chain, with identical relative energy values, four of them displaying opposite orientations of the ring OH's. As to the *S-trans* geometries, ten were calculated for MC, nine for EC, while only five were found for IPC (also as compared to the analogous propyl caffeate, PC), on account of destabilizing steric factors between the bulkier isopropyl group and the neighbor (C)H atoms (Fig. 7). This also explains the lower number of conformers yielded for IPC, as well as the slightly higher $\Delta E_{S-trans-cis}$ obtained for IPC: $\Delta E_{S-trans-cis} = 14.5$ kJ mol⁻¹ versus 12.7 and 11.7 kJ mol⁻¹ for MC and EC, respectively.

Since this type of phenolic compounds exert their biological action at physiological conditions, the effect of the solvent (water) on their structural behavior was verified by performing Self-Consistent Reaction Field (SCRF) calculations for the most stable geometries (population $\geq 10\%$) of the smallest elements of the series (MC, EC and IPC). The results obtained allowed to us to conclude that the presence of water does not significantly affect either the conformational preferences or the stability order of these systems, thus enabling the extrapolation of the results obtained in the gaseous phase to the aqueous medium.

The lowest energy geometries presently calculated for these dihydroxycinnamic alkyl esters are in good accor-

dance with previously reported results for caffeic acid, obtained both by theoretical [30] and X-ray methods [32] (Table 1). Esterification was found to lead to a higher number of geometries displaying an opposite orientation of the ring hydroxyl groups (although not populated at room temperature), since for the parent acid only one such conformation was found to be an energy minimum. Indeed, substitution of the carboxylic OH for an ester alkyl group allows for a higher conformational freedom, as long as the alkyl hydrogens display a staggered conformation relative to the neighbor H(C) atom (Figs. 3, 5 and 7). This yields a larger number of conformers for the esters as compared to the acid (for which 11 minima were obtained [30]).

The theoretical vibrational spectra (both Raman and infrared) of the esters studied were obtained. Table 2 contains the harmonic wavenumbers calculated for the lowest energy conformers of MC, EC and IPC (along with a preliminary assignment), evidencing a quite good overall accordance with the values reported for caffeic acid [30] and other similar systems [11, 31]. These calculated frequencies will allow a complete assignment of the experimental Raman spectra of the systems (both in the solid state and in aqueous solution), which are to be published in the near future (manuscript in preparation).

Summary

For the series of cinnamic esters investigated, the most stable geometries correspond to planar arrangements displaying an identical orientation of the aromatic hydroxyl

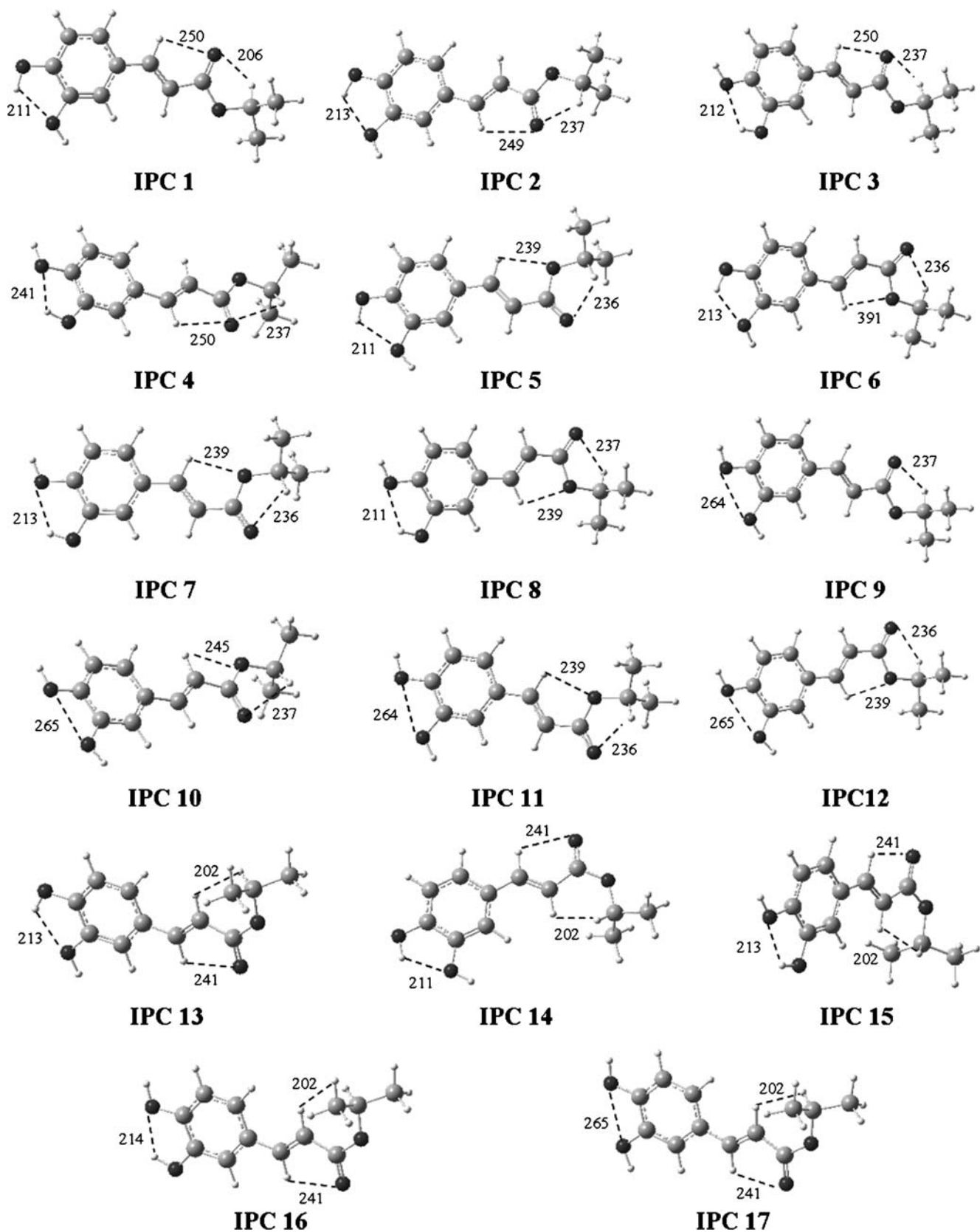


Fig. 7 Representation of the several conformers calculated for IPC-displaying (C)H \cdots O and (O)H \cdots O intramolecular interactions. B3LYP/6-31G** level of calculation. Intramolecular distances are represented in pm

Table 1 Calculated optimized geometries and dipole moments for the most stable conformer of MC, EC and IPC. B3LYP/6-31G** level of calculation

$^a\mu$ (D)	c CA1	MC 1	EC 1	IPC 1
	3.5	3.5	3.7	3.6
Bond lengths (pm)				
b O ₇ –C ₆	137.5	135.7	135.7	135.7
O ₈ –C ₅	121.8	137.5	137.6	137.6
O ₁₂ –C ₁₁	136.2	121.8	121.8	121.9
O ₁₃ –C ₁₁	–	135.9	135.8	135.8
O ₁₃ –C ₂₁	139.2	143.3	145.3	145.5
C ₁ –C ₆	139.3	139.2	139.2	139.2
C ₂ –C ₁	140.5	139.3	139.3	139.3
C ₃ –C ₂	141.3	140.5	140.5	140.5
C ₄ –C ₃	138.5	141.2	141.2	141.2
C ₅ –C ₄	141.2	138.2	138.3	138.3
C ₆ –C ₅	145.6	141.1	141.1	141.1
C ₃ –C ₉	134.8	145.7	145.7	145.7
C ₉ –C ₁₀	147.0	134.7	134.7	134.7
C ₁₀ –C ₁₁	97.0	147.3	147.4	147.4
C ₂₁ –C ₂₄	–	–	151.7	152.2
C ₂₁ –C ₂₃	–	–	–	152.6
O ₇ –H ₁₈	96.5	97.0	97.0	97.0
O ₈ –H ₁₇	97.2	96.5	96.5	96.5
O ₁₃ –H ₂₁	108.5	–	–	–
C ₁ –H ₁₄	108.6	108.4	108.4	108.4
C ₂ –H ₁₅	108.7	108.5	108.6	108.6
C ₄ –H ₁₆	108.9	108.7	108.7	108.7
C ₉ –H ₁₉	108.5	108.9	108.9	108.9
C ₁₀ –H ₂₀	–	108.5	108.5	108.5
C ₂₁ –H ₂₂	–	109.3	109.5	109.4
C ₂₁ –H ₂₃	–	109.3	109.5	–
C ₂₁ –H ₂₄	135.6	109.0	–	–
C ₂₄ –H ₂₅	–	–	109.4	109.3
C ₂₄ –H ₂₆	–	–	109.4	109.4
C ₂₄ –H ₂₇	–	–	109.4	109.5
C ₂₃ –H ₂₈	–	–	–	109.5
C ₂₃ –H ₂₉	–	–	–	109.2
C ₂₃ –H ₃₀	–	–	–	109.5
Bond angles (degrees)				
O ₁₂ –C ₁₁ –O ₁₃	121.9	123.0	123.2	123.8
O ₇ –C ₆ –C ₁	120.4	120.4	120.4	120.4
O ₈ –C ₅ –C ₄	124.9	124.8	124.8	124.8
O ₁₂ –C ₁₁ –C ₁₀	126.6	126.3	126.1	125.7
O ₁₃ –C ₁₁ –C ₁₀	111.5	110.7	110.7	110.5
C ₂₁ –O ₁₃ –C ₁₁	–	115.0	115.6	117.0
O ₁₃ –C ₂₁ –C ₂₄	–	–	107.5	106.0
O ₁₃ –C ₂₁ –C ₂₃	–	–	–	107.9
C ₃ –C ₂ –C ₁	121.5	121.5	121.5	121.5
C ₄ –C ₃ –C ₂	118.1	118.1	118.1	118.1
C ₅ –C ₄ –C ₃	120.5	120.5	120.5	120.5
C ₆ –C ₁ –C ₂	119.9	119.9	119.9	119.9
C ₉ –C ₃ –C ₄	122.4	122.9	122.9	122.9
C ₁₀ –C ₉ –C ₃	128.2	128.1	128.2	128.1
C ₁₁ –C ₁₀ –C ₉	120.0	120.1	120.1	120.2
C ₅ –O ₈ –H ₁₇	110.1	110.1	110.0	107.4
C ₆ –O ₇ –H ₁₈	107.7	107.7	107.7	110.0
C ₁₁ –O ₁₃ –H ₂₁	105.5	–	–	–

Table 1 (continued)

$^a\mu$ (D)	c CA1	MC 1	EC 1	IPC 1
	3.5	3.5	3.7	3.6
O ₁₃ –C ₂₁ –H ₂₂	–	110.8	109.0	107.7
O ₁₃ –C ₂₁ –H ₂₃	–	110.8	109.0	–
O ₁₃ –C ₂₁ –H ₂₄	–	105.8	–	–
C ₂ –C ₁ –H ₁₄	121.5	121.4	121.4	121.4
C ₃ –C ₂ –H ₁₅	119.1	119.1	119.1	119.1
C ₅ –C ₄ –H ₁₆	119.2	119.2	119.2	119.2
C ₃ –C ₉ –H ₁₉	115.8	115.8	115.8	115.8
C ₉ –C ₁₀ –H ₂₀	123.3	123.3	123.3	123.3
C ₂₁ –C ₂₄ –H ₂₅	–	–	109.9	110.8
C ₂₁ –C ₂₄ –H ₂₆	–	–	110.9	110.1
C ₂₁ –C ₂₄ –H ₂₇	–	–	110.9	110.8
C ₂₁ –C ₂₃ –H ₂₈	–	–	–	110.6
C ₂₁ –C ₂₃ –H ₂₉	–	–	–	110.4
C ₂₁ –C ₂₃ –H ₃₀	–	–	–	110.2
H ₂₂ –C ₂₁ –H ₂₃	–	108.5	107.2	–
H ₂₂ –C ₂₁ –H ₂₄	–	110.5	–	–
H ₂₅ –C ₂₄ –H ₂₆	–	–	108.3	108.4
H ₂₅ –C ₂₄ –H ₂₇	–	–	108.3	108.3
H ₂₈ –C ₂₃ –H ₂₉	–	–	–	109.0
H ₂₈ –C ₂₃ –H ₃₀	–	–	–	108.3
Dihedral angles (degrees)				
O ₁₂ –C ₁₁ –O ₁₃ –C ₂₁	–	0.0	0.0	–0.1
O ₇ –C ₆ –C ₁ –C ₂	–180.0	180.0	180.0	–180.0
O ₈ –C ₅ –C ₄ –C ₃	–180.0	–180.0	180.0	180.0
O ₁₂ –C ₁₁ –C ₁₀ –C ₉	0.0	0.0	0.0	–0.2
O ₁₃ –C ₁₁ –C ₁₀ –C ₉	–180.0	–179.9	180.0	180.0
C ₂₁ –O ₁₃ –C ₁₁ –C ₁₀	–	179.9	180.0	179.7
C ₁₁ –O ₁₃ –C ₂₁ –C ₂₄	–	–	180.0	–153.5
C ₁₁ –O ₁₃ –C ₂₁ –C ₂₃	–	–	–	83.6
C ₁ –C ₂ –C ₃ –C ₄	0.0	0.0	0.0	0.0
C ₅ –C ₄ –C ₃ –C ₂	0.0	0.0	0.0	0.0
C ₆ –C ₁ –C ₂ –C ₃	0.0	0.0	0.0	0.0
C ₉ –C ₃ –C ₄ –C ₅	–180.0	–180.0	180.0	180.0
C ₁₀ –C ₉ –C ₃ –C ₄	0.0	0.0	–180.0	–0.1
C ₁₁ –C ₁₀ –C ₉ –C ₃	180.0	–180.0	–180.0	180.0
C ₁ –C ₆ –O ₇ –H ₁₈	180.0	180.0	180.0	180.0
C ₄ –C ₅ –O ₈ –H ₁₇	0.0	0.0	0.0	0.0
C ₁₀ –C ₁₁ –O ₁₃ –H ₂₁	180.0	–	–	–
C ₁₁ –O ₁₃ –C ₂₁ –H ₂₂	–	–60.2	58.3	–35.1
C ₁₁ –O ₁₃ –C ₂₁ –H ₂₃	–	60.2	–58.3	–
C ₁₁ –O ₁₃ –C ₂₁ –H ₂₄	–	180.0	–	–
O ₁₃ –C ₂₁ –C ₂₄ –H ₂₅	–	–	–180.0	58.5
O ₁₃ –C ₂₁ –C ₂₄ –H ₂₆	–	–	60.2	178.5
O ₁₃ –C ₂₁ –C ₂₄ –H ₂₇	–	–	–60.2	–61.8
O ₁₃ –C ₂₁ –C ₂₃ –H ₂₈	–	–	–	59.1
O ₁₃ –C ₂₁ –C ₂₃ –H ₂₉	–	–	–	–61.6
O ₁₃ –C ₂₁ –C ₂₃ –H ₃₀	–	–	–	178.8
C ₃ –C ₂ –C ₁ –H ₁₄	180.0	–180.0	180.0	180.0
C ₄ –C ₃ –C ₂ –H ₁₅	180.0	180.0	180.0	–180.0
C ₆ –C ₅ –C ₄ –H ₁₆	180.0	–180.0	–180.0	–180.0
C ₄ –C ₃ –C ₉ –H ₁₉	–180.0	–180.0	–180.0	179.8
C ₃ –C ₉ –C ₁₀ –H ₂₀	0.0	0.0	0.0	–0.1

^aTotal dipolar moment 1D=1/3×10^{–2} Cm^bAtoms are numbered according to Fig. 1a^c[30]

groups (coplanar with the ring), an *S-cis* conformation of the ester group with respect to C=O, and an *anti* relative position of the carbonyl and ring OH's, coupled to (C₂C₃C₉C₁₀) and (C₉C₁₀C₁₁O₁₂) dihedrals equal to 180°

and 0°, respectively. The preference for planarity is expected, since it favors electron delocalization through the expanded π system of the hyperconjugated molecules of this type of hydroxycinnamic systems. Thus, non-planar

Table 2 Calculated vibrational wavenumbers (cm⁻¹) for the most stable conformer of MC, EC and IPC. B3LYP/6-31G** level of calculation

CAM 1	CAE 1	CAIP 1	^b Approximate description
3,694 ^a (59;97)	3,693 (58;95)	3,693 (58;94)	ν (O ₈ H)
3,628 (126;176)	3,628 (125;178)	3,628 (126;183)	ν (O ₇ H)
3,094 (7;175)	3,094 (7;179)	3,094 (7;181)	$\nu_{\text{as}}(\text{CH})_{\varphi}$
3,081 (12;34)	3,081 (12;32)	3,080 (12;31)	ν (CH) _{chain}
3,073 (5;61)	3,071 (5;62)	3,071 (5;62)	$\nu_{\text{as}}(\text{CH})_{\varphi}$
3,057 (7;24)	3,055 (7;23)	3,055 (7;23)	$\nu_{\text{as}}(\text{C}_4\text{H}_{16})_{\varphi}$
3,048 (3;31)	3,047 (1;23)	3,047 (1;29)	ν (CH) _{chain}
3,047 (20;99)			$\nu_{\text{as}}(\text{CH}_3)+\nu(\text{CH})_{\text{chain}}$
	3,015 (38;29)		$\nu_{\text{as}}(\text{CH}_3)+\nu_{\text{as}}(\text{CH}_2)$
3,013 (24;68)	3,008 (28;125)	3,025 (17;45)	$\nu_{\text{as}}(\text{CH}_3)$
		3,010 (26;61)	$\nu_{\text{as}}(\text{CH}_3)+\nu(\text{C}_{21}\text{H})$
		3,007 (6;57)	$\nu_{\text{as}}(\text{CH}_3)+\nu(\text{C}_{21}\text{H})$
		2,998 (6;4)	$\nu_{\text{as}}(\text{CH}_3)$
	2,979 (10;86)		$\nu_{\text{as}}(\text{CH}_3)+\nu_{\text{as}}(\text{CH}_2)$
		2,967 (2;65)	$\nu(\text{C}_{21}\text{H})$
	2,942 (21;124)		$\nu_{\text{s}}(\text{CH}_2)$
2,942 (49;202)	2,936 (21;153)	2,934 (27;290)	$\nu_{\text{s}}(\text{CH}_3)$
		2,930 (14;4)	$\nu_{\text{s}}(\text{CH}_3)$
1,724 (194;78)	1,721 (192;69)	1,714 (179;61)	$\nu(\text{C}=\text{O})$
1,630 (197;980)	1,630 (195;1046)	1,629 (199;1111)	$\nu(\text{C}=\text{C})_{\text{chain}}$
1,599 (246;1758)	1,599 (248;1889)	1,599 (258;2061)	φ 8a+ $\nu(\text{C}=\text{C})_{\text{chain}}$
1,584 (26;14)	1,585 (27;15)	1,582 (26;15)	φ 8b+ $\delta(\text{O}_7\text{H})$
1,511 (177;3)	1,512 (178;3)	1,512 (181;3)	φ 19a+ $\delta(\text{O}_8\text{H})$
	1,474 (4;6)		$\delta_{\text{as}}(\text{CH}_3)+\text{sciss}(\text{CH}_2)$
	1,454 (2;23)		$\delta_{\text{as}}(\text{CH}_3)+\text{sciss}(\text{CH}_2)$
1,453 (9;23)		1,467 (8;3)	$\delta_{\text{as}}(\text{CH}_3)$
1,436 (5;29)		1,453 (3;36)	$\delta_{\text{as}}(\text{CH}_3)$
	1,443 (5;25)	1,444 (2;32)	$\delta_{\text{as}}(\text{CH}_3)$
		1,438 (1;2)	$\delta_{\text{as}}(\text{CH}_3)$
1,435 (178;172)	1,435 (173;177)	1,435 (177;192)	φ 19b + $\delta(\text{OH})_{\varphi}$
1,424 (19;2)		1,377 (5;9)	$\delta_{\text{s}}(\text{CH}_3)$
	1,383 (9;9)		$\delta_{\text{s}}(\text{CH}_3)+\omega(\text{CH}_2)$
1,373 (92;27)	1,373 (101;25)	1,374 (109;20)	$\delta(\text{O}_7\text{H})+(\text{CH})_{\text{chain}}+\varphi$ 19b+ $\delta_{\text{s}}(\text{CH}_3)$
		1,362 (20;7)	$\delta_{\text{s}}(\text{CH}_3)+\delta(\text{C}_{21}\text{H})$
	1,349 (1;2)		$\omega(\text{CH}_2)+\delta_{\text{s}}(\text{CH}_3)+\delta(\text{O}_7\text{H})$
		1,342 (5;17)	$\delta(\text{C}_{21}\text{H})+\delta_{\text{s}}(\text{CH}_3)+\delta(\text{O}_7\text{H})+(\text{CH})_{\text{chain}}$
		1,321 (21;11)	$\delta(\text{C}_{21}\text{H})+\delta_{\text{s}}(\text{CH}_3)+\delta(\text{O}_7\text{H})+(\text{CH})_{\text{chain}}$
1,316 (20;26)	1,315 (10;38)	1,314 (1;36)	φ 3 + $\delta(\text{CH})_{\text{chain}} + \delta(\text{OH})_{\varphi}$
1,305 (65;55)			φ 14+ $\delta(\text{CH})_{\text{chain}}+\delta(\text{O}_8\text{H})$
	1,301 (85;50)		φ 14+ $\delta(\text{CH})_{\text{chain}}+\delta(\text{O}_8\text{H})+\omega(\text{CH}_2)$
		1,298 (62;63)	φ 14+ $\delta(\text{CH})_{\text{chain}}+\delta(\text{O}_8\text{H})+\delta(\text{C}_{21}\text{H})$
1,294 (13;2)	1,292 (22;5)	1,291 (25;17)	$\nu(\text{CH})_{\text{chain}}+\delta(\text{O}_8\text{H})$
1,272 (461;11)	1,272 (484;9)	1,271 (480;8)	$\nu(\text{C}_6\text{O})+\delta(\text{CH})+\delta(\text{OH})+18\text{b}$
	1,246 (0;17)		t (CH ₂)
1,233 (20;66)	1,233 (21;61)	1,233 (19;60)	$\delta(\text{CH})_{\text{chain}}+\delta(\text{O}_7\text{H})+\varphi$ 3
1,172 (281;213)	1,172 (252;206)	1,172 (247;217)	$\delta(\text{CH})_{\text{chain}}+\delta(\text{O}_7\text{H})+\varphi$ 18a
		1,163 (4;2)	r (CH ₃)+ $\delta(\text{CH})_{\text{chain}}$
1,169 (178;52)		1,154 (535;192)	$\nu(\text{C}_{11}\text{O})+\delta(\text{CH})_{\text{chain}}$
	1,154 (678;206)		$\nu(\text{C}_{11}\text{O})+\delta(\text{CH})_{\text{chain}}$
1,155 (406;140)			$\delta(\text{CH})_{\text{chain}}+\nu(\text{OC})+r(\text{CH}_3)$

Table 2 (continued)

CAM 1	CAE 1	CAIP 1	^b Approximate description
1,144 (105;177)	1,145 (195;247)	1,144 (176;265)	φ 18b+ δ (OH)+ δ (CH) _{chain}
	1,139 (4;2)		r (CH ₃)+r (CH ₂)
1,133 (1;6)			r (CH ₃)
1,129 (121;8)	1,129 (119;6)	1,130 (108;3)	φ 18a+ δ (O ₈ H)
		1,123 (10;4)	r (CH ₃)
		1,103 (333;33)	r (CH ₃)+ ν (C ₂₁ O ₁₃)
	1,098 (4;9)		r (CH ₃)+ ν (C ₂₁ C ₂₄)
1,092 (82;8)	1,091 (83;13)	1,091 (85;14)	φ 18a+ δ (OH)
1,014 (12;26)	1,029 (56;5)		ν (CO ₁₃)+ ν (C ₂₁ C)
992 (22;3)	992 (22;3)	992 (21;3)	γ (CH) _{chain}
958 (1;5)	965 (2;5)	981 (15;8)	φ 18b
		953 (10;3)	φ 7b
911 (16;4)	947 (8;3)		ν (CC)+ ν (CO)+ ν (OC)+ φ 7b
		919 (2;4)	r (CH ₃)
906 (2;4)	907 (1;4)	907 (1;4)	γ_{as} (CH) α
		905 (1;4)	r (CH ₃)
	861 (6;14)	890 (16;5)	r (CH ₃)
844 (4;11)	844 (3;11)	844 (3;11)	γ (CH) _{chain} + φ 11
810 (45;1)	810 (43;1)	810 (39;1)	φ 11
		810 (6;11)	r (CH ₃) + γ (CH) ϕ
796 (11;7)	797 (11;7)	796 (12;7)	φ 10a
785 (3;44)	788 (1;47)	786 (3;63)	φ 12+ ν (O ₇ C)
	781 (2;0)		r (CH ₃)+r (CH ₂)
750 (10;4)	760 (10;6)	760 (9;6)	φ 12+ Δ (CO ₁₃ C)
710 (2;1)	709 (2;1)	710 (2;1)	Γ (OCO)+ φ 5
693 (7;22)	701 (8;12)	698 (7;11)	φ 6a+ Δ (OCO)
663 (1;0)	663 (0;0)	663 (1;0)	φ 4
584 (7;1)	584 (7;1)	585 (7;1)	φ 16b
578 (29;6)	579 (29;6)	578 (30;6)	φ 6b
531 (10;2)	528 (12;2)	529 (9;2)	δ (CC) _{chain} + φ 6a
496 (14;1)	499 (11;2)	500 (13;2)	φ 6b+ δ (CC) _{chain}
		462 (4;1)	Δ (CCC)
450 (67;3)	449 (64;3)	449 (64;3)	γ (O ₇ H)
435 (2;1)	437 (5;1)		Δ (CCC)
		428 (11;1)	φ 16a+ γ (O ₇ H)
427 (13;0)	427 (15;0)	426 (6;1)	φ 16a+ γ (O ₇ H)
		402 (10;1)	Γ (C ₂₁ C ₂₃ C ₂₄)
398 (3;2)	397 (3;1)	396 (2;2)	Γ (CCC)
		356 (4;1)	Γ (C ₂₁ C ₂₃ C ₂₄)
334 (28;2)	380 (5;1)		Δ (CO ₁₃ C)
314 (3;0)	314 (4;0)	314 (4;0)	δ (COH) _{ring}
261 (6;2)	299 (17;2)		Δ (CCC)
	274 (0;0)	280 (11;2)	τ (CH ₃)
261 (4;2)			Γ (CCH)+ Γ (CO ₈ H)
	257 (9;3)	259 (9;3)	Γ (CCH)+ Γ (CO ₈ H)+ τ (CH ₃)
		256 (2;1)	τ (CH ₃)
223 (140;3)	228 (143;2)	229 (143;1)	γ (O ₈ H)
		224 (0;0)	τ (CH ₃)
	217 (0;4)	213 (1;3)	Δ (CCC)
213 (7;2)			Δ (CC) _{chain} + γ (O ₈ H)+ Γ (COC)
193 (2;3)	196 (7;0)	195 (10;0)	τ (CH ₃)+ Γ (CCH)+ Γ (COH)
	185 (6;3)	170 (2;3)	Longitudinal skeleton mode
192 (16;1)	161 (3;1)	154 (2;2)	τ (CH ₃)+ Γ (CCC)
109 (0;1)			Skeleton mode
97 (2;1)	95 (2;1)	83 (2;0)	τ (CH ₃)
			Skeleton mode

Table 2 (continued)

CAM 1	CAE 1	CAIP 1	^b Approximate description
	60 (0;1)	73 (0;1)	Skeleton mode
70 (0;0)	56 (0;1)	55 (0;1)	Skeleton mode
60 (0;1)	56 (0;0)	40 (0;2)	Skeleton mode
31 (0;1)	24 (0;3)	25(0;3)	Skeleton mode

^aIR intensities in km.mol⁻¹; Raman scattering activities in Å.amu⁻¹

^bAtoms are numbered according to Fig. 1a.

The Wilson's notation was used for descriptions of benzene derivatives normal vibrations [33, 34]: for in-plane vibrations: C-C stretching vibrations (8a, 8b, 14, 19a, 19b), C-H/X bending vibrations (3, 18a, 18b), radial skeletal vibrations (6a, 6b, 12), C-H stretching vibrations (7a, 7b); for out-of-plane vibrations: C-H/X vibrations (5, 10a, 11), skeletal vibrations (16a, 16b)

δ: in-plane deformation; t: twisting; r: rocking; ω: wagging; sciss.: scissoring; γ: out-of-plane deformation; Δ: in-plane deformation skeleton atoms; Γ: out-of-plane deformation skeleton atoms

geometries (in the ester alkyl moiety) arise only in order to overcome steric hindrance destabilizing factors (such as H ⋯ H interactions). The additional degrees of freedom introduced by esterification are mainly reflected in the internal rotation around the C₁₁–O₁₃ bond, defining either a *S-cis* or a *S-trans* conformation, which was shown to be the most important factor determining the overall stability of these phenolic systems. In fact, esterification is expected to affect mainly the energy barrier corresponding to the (O=) C-OR internal rotation.

The conformational results presently obtained are in perfect agreement with reported data on similar di- and trihydroxylated cinnamic acids and esters, namely *trans*-caffeic acid (3-(3,4-dihydroxyphenyl)-2-propenoic acid) [30], *trans*-3-(3,4,5-trihydroxyphenyl)-2-propenoic acid [31] and *trans*-ethyl 3-(3,4,5-trihydroxyphenyl)-2-propenoate [11]. Also, the present results are corroborated by preliminary structural data gathered for some elements of this type of phenolic esters [31].

This kind of conformational study based on theoretical methods is of the utmost relevance for future studies aiming at the elucidation of the structure–activity relationships (SARs) ruling the biological function of phenolic compounds with potential chemopreventive and/or chemotherapeutic properties, and at a better understanding of the mechanisms underlying this activity. Moreover, quantum mechanical studies such as the ones presently reported yield highly accurate structural data, as compared to semiempirical or force field approaches normally used in the construction of SAR and QSAR (quantitative structure–activity relationships) models. In fact, development of such a model requires a thorough knowledge of the most stable conformers for each element of the homologous series of compounds investigated (directly related to a leader, e.g., the parent acid), in order for their structural parameters to be used as reliable descriptors. For the phenolic derivatives under study, only those conformers with population at room temperature above 20%—geometries 1 and 2—should be considered for a QSAR model.

Cytotoxicity evaluation of the phenolic compounds presently discussed against distinct human cancer cell lines is underway in our laboratory (concomitantly with the structural elucidation of the compounds tested), promising results having already been obtained [3, 10, 31]. A combined analysis of the structural and biological data will yield reliable SARs and QSARs, thus contributing to the wider goal of developing new and more effective chemopreventive and/or chemotherapeutic agents.

Acknowledgements The authors acknowledge financial support from the Portuguese Foundation for Science and Technology (FCT) – Project POCI/QUI/55631/2004 (co-financed by the European Community fund FEDER). R.C. and S.M.F. thank FCT for PhD fellowships SFRH/BD/16520/2004 and SFRH/BD/17493/2004.

References

- Koo KA, Kim SH, Oh TH, Kim YC (2006) Life Sciences 79:709–716 DOI 10.1016/j.lfs.2006.02.019
- Fresco P, Borges F, Diniz C, Marques MPM (2006) Med Res Rev 26:747–766 DOI 10.1002/med.20060
- Marques MPM, Borges F, Sousa JB, Calheiros R, Garrido J, Gaspar A, Antunes F, Diniz C, Fresco P (2006) Lett Drug Design Dev 3:316–320 DOI 10.2174/157018006777574212
- Shin KM, Kim IT, Park YM, Ha J, Choi JW, Park HJ, Lee YS, Lee KT (2004) Biochem Pharmacol 68:2327–2336 DOI 10.1016/j.bcp.2004.08.002
- Silva FAM, Borges F, Guimarães C, Lima JLFC, Matos C, Reis S (2000) J Agric Food Chem 48:2122–2126 DOI 10.1021/jf9913110
- Siquet C, Paiva-Martins F, Lima JL, Reis S, Borges F (2006) Free Radic Res 40:433–442 DOI 10.1080/10715760500540442
- Que F, Mao L, Pan X (2006) Food Res Int 39:581–587 DOI 10.1016/j.foodres.2005.12.001
- Cárdenas M, Marder M, Blank VC, Roguin LP (2006) Bioorg Med Chem 14:2966–2971 DOI 10.1016/j.bmc.2005.12.021
- Fiuza SM, Besien EV, Milhazes N, Borges F, Marques MPM (2004) Bioorg Med Chem 12:3581–3589 DOI 10.1016/j.bmc.2004.04.026
- Gomes CA, Girão da Cruz T, Andrade JL, Milhazes N, Borges F, Marques MPM (2003) J Med Chem 46:5395–5401 DOI 10.1021/jm030956v
- Sousa JB, Calheiros R, Rio V, Borges F, Marques MPM (2006) J Mol Struct 783:122–135 DOI 10.1016/j.molstruc.2005.09.004

12. Sergediene E, Jonsson K, Szymusiak H, Tyrakowska B, Rietjens IMCM, Cenas N (1999) FEBS Lett 462:392–396 DOI 10.1016/S0014-5793(99)01561-6
13. Hwang HJ, Park HJ, Chung HJ, Min HY, Park EJ, Hong JY, Lee SK (2006) J Nutr Biochem 17:356–362 DOI 10.1016/j.jnutbio.2005.08.009
14. Chen YJ, Shiao MS, Wang SY (2001) Anticancer Drugs 12:143–149
15. Lee YJ, Liao PH, Chen WK, Yang CY (2000) Cancer Lett 153:51–56 DOI 10.1016/S0304-3835(00)00389-X
16. Kuo HC, Kuo WH, Lee YJ, Lin WL, Chou FP, Tseng TH (2006) Cancer Lett 234:199–208 DOI 10.1016/j.canlet.2005.03.046
17. Nichenametla SN, Taruscio TG, Barney DL, Exon JH (2006) Crit Rev Food Sci Nut 46:161–183 DOI 10.1080/10408390591000541
18. Frisch MJ et al (2003) Gaussian 03, Revision B.04, Gaussian, Pittsburgh PA, USA
19. Lee C, Yang W, Parr RG (1988) Phys Rev B37:785–789 DOI 10.1103/PhysRevB.37.785
20. Miehllich B, Savin A, Stoll H and Preuss H (1989) Chem Phys Lett 157:200–206 DOI 10.1016/0009-2614(89)87234-3
21. Becke A (1988) Phys Rev A38:3098–3100 DOI 10.1103/PhysRevA.38.3098
22. Becke AJ (1993) J Chem Phys 98:5648–5652 DOI 10.1063/1.464913
23. Petersson GA, Bennett A, Tensfeldt TG, Al-Laham MA, Shirley WA, Mantzaris J (1988) J Chem Phys 89:2193–2218 DOI 10.1063/1.455064
24. Peng C, Ayala PY, Schlegel HB, Frisch MJ (1996) Comp Chem 17:49–56 DOI 10.1002/(SICI)1096-987X(19960115)17:1<49::AID-JCC5>3.0.CO;2-0
25. Cancés E, Mennucci B, Tomasi J (1997) J Chem Phys 107:3032–3041 DOI 10.1063/1.474659
26. Mennucci B, Cancés E, Tomasi J (1997) J Phys Chem B 101:10506–10517 DOI 10.1021/jp971959k
27. Cancés E, Mennucci B (1998) J Math Chem 23:309–326 DOI 10.1023/A:1019133611148
28. Cammi R, Tomasi J (1995) J Comp Chem 16:1449–1458 DOI 10.1002/jcc.540161202
29. Barone V, Cossi M, Tomasi J (1998) J Comp Chem 19:404–417 DOI 10.1002/(SICI)1096-987X(199803)19:4<404::AID-JCC3>3.0.CO;2-W
30. VanBesien E, Marques MPM (2003) J Mol Struct (THEOCHEM) 625:265–275 DOI 10.1016/S0166-1280(03)00026-5
31. Fiuza SM, Besien EV, Milhazes N, Borges F, Marques MPM (2004) J Mol Struct 693:103–118 DOI 10.1016/j.molstruc.2004.02.019
32. García-Granda S, Beurskens G, Beurskens PT, Krishna TSR, Desiraju GR (1987) Acta Cryst C43:683–685 DOI 10.1107/S0108270187094526
33. Wilson EB Jr (1934) Phys Rev 45:706–714 DOI 10.1103/PhysRev.45.706
34. Varsányi G (1974) Assignments for vibrational spectra of seven hundred benzene derivatives, Akadémiai Kiadó, Budapest/Adam Hilger, London